Title: Thermomechanical coupling shapes the Antarctic Ice Sheet's internal structure

Authors: Xiao Xiao[1], Lianxing Wen[2] and Ping Tong[1,3,4*]

Affiliations:

[1]Division of mathematical Sciences, School of Physical and Mathematical Sciences, Nanyang Technological University, Singapore

[2]Department of Geosciences, State University of New York at Stony Brook, Stony Brook, NY, USA

[3]Earth Observatory of Singapore, Nanyang Technological University, Singapore

[4]Asian School of the Environment, Nanyang Technological University, Singapore

[*]Corresponding authors: Ping Tong (tongping@ntu.edu.sg)

Overview

The Supplementary Information includes 1 note, 3 figures and 5 tables

List

- Supplementary Note 1: Inversion for TTI anisotropy in the lower ice
- Supplementary Figure 1: Receiver function (RF) harmonic decomposition analysis at representative stations.
- Supplementary Figure 2: Harmonic fitting for *Pbp* travel time from autocorrelation function (ACF) at representative Antarctic seismic stations.
- Supplementary Figure 3: Synthetic seismic properties of endmember models and inversion for lower ice dipping anisotropy.
- Supplementary Table 1: Detailed information for 181 seismic stations in study region
- Supplementary Table 2: Observed *PbP* arrival times from ACF
- Supplementary Table 3: MCMC parameters in inversion for 2D seismic structure
- Supplementary Table 4: Bulk-ice seismic structures across stations
- Supplementary Table 5: Lower-ice seismic anisotropic structures across stations

Supplementary Note 1: Inversion for TTI anisotropy in the lower ice

Tilted Transverse Isotropy (TTI) anisotropy in the lower ice, parameterized by equivalent melt fraction (EMF; ε) and dip inclination (α), is estimated via a grid search to best match the isotropic *Vp/Vs* and *Vs* azimuthal anisotropy derived from the MCMC inversion (Supplementary Fig. 4b). The misfit function is defined as

$$\varphi = \varphi_P + \varphi_\zeta = \left(\frac{P_{TTI}(\varepsilon,\alpha) - P_{obs}}{\delta P}\right)^2 + \left(\frac{\zeta_{TTI}(\varepsilon,\alpha) - \zeta_{obs}}{\delta \zeta}\right)^2 \quad (1)$$

where φ_P and φ_ζ are the L2-norm misfits between synthetic and observed *Vp/Vs* and *Vs* azimuthal anisotropy, respectively, weighted by their uncertainties (δP and $\delta\zeta$). Synthetic values $P_{TTI}(\varepsilon,\alpha)$ and $\zeta_{TTI}(\varepsilon,\alpha)$ are evaluated for each model, and compared with observations P_{obs} and ζ_{obs}. The parameter space is explored over $\varepsilon = 0.0 – 2.0$ (step 0.01) and $\alpha = 0 – 90°$ (step 1°). The EMF arising from the combined effects of CPO and intergranular water is defined as $\varepsilon = \frac{\psi}{V}\sum_{r=1}^{N} l_r A_r$, where N is the number of microcracks (including intergranular boundaries and water-filled veins), l_r is the length of the r-th grain boundary, A_r is cross-sectional area of the minor cracks, ψ is the crack aspect ratio (assumed to be 10^{-3}), and V is the representative elementary volume[26]. The inclination α is the angle between the grain c-axes and the vertical. Observed lower-ice *Vp/Vs* and anisotropy are inferred from seismic results by assuming that the uppermost one-third of the ice column is isotropic, with pure ice elastic properties (bulk modulus $K_0 = 9.2$ Gpa, shear modulus $\mu_0 = 3.6$ Gpa, and density $\rho = 9.17$ kg/m^3). For upward-propagating waves, synthetic *Vp/Vs* (P_{TTI}) and *Vs* azimuthal anisotropy (ζ_{TTI}) of a TTI anisotropic ice are calculated as

$$P_{TTI} = \frac{Vp_{TTI}^{fast} + Vp_{TTI}^{slow}}{Vs_{TTI}^{fast} + Vs_{TTI}^{slow}}, \zeta_{inc} = \frac{2\left(Vs_{TTI}^{fast} - Vs_{TTI}^{slow}\right)}{Vs_{TTI}^{fast} + Vs_{TTI}^{slow}} \quad (2)$$

where V^{fast} and V^{slow} denote azimuthal fast and slow seismic velocities. These velocities are expressed as mixtures of vertical (VTI) and horizontal (HTI) transverse isotropy:

$$V_{TTI} = V_{\mathrm{VTI}}(\varepsilon)\cdot cos^2(\alpha) + V_{\mathrm{HTI}}(\varepsilon)\cdot sin^2(\alpha) \quad (3)$$

where V_{TTI} represents either *Vp* or *Vs*, and V_{VTI} and V_{HTI} are the corresponding velocities for the VTI and HTI models. For small crack aspect ratios, *P*-wave velocities are azimuthal isotropy[27]:

$$Vp_{VTI}^{fast} = Vp_{VTI}^{slow} = Vp_{HTI}^{fast} = Vp_{HTI}^{slow} = \sqrt{\frac{K_0 + 4\mu_0/3}{\rho}} \quad (4)$$

whereas *S*-wave velocities follows:

$$Vs_{VTI}^{fast} = Vs_{VTI}^{slow} = Vs_{HTI}^{slow} = \sqrt{\frac{\mu_0/(1+\varepsilon)}{\rho}},\ Vs_{HTI}^{fast} = \sqrt{\frac{\mu_0}{\rho}} \quad (5)$$

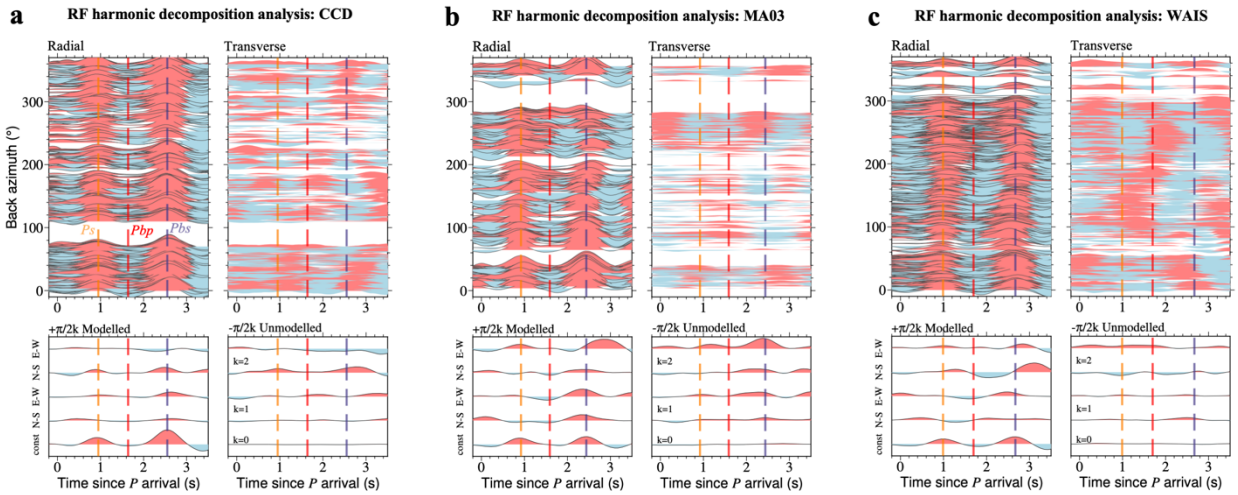

Supplementary Fig. 1 | RF harmonic decomposition analysis at representative stations. a, Station **CCD**. Top, radial (left) and transverse (right) RFs as a function of tele-seismic back-azimuth (positive amplitudes in red, negative in blue). Bottom, modelled (left) and residual (unmodelled; right) harmonic components. The decomposition result includes five harmonics: one zeroth-order (isotropic) component ($k = 0$); two first-order components ($k = 1$; east-west and north-south directions), with 2π back-azimuthal periodicity; and two second-order components ($k = 2$; east-west and north-south directions), with π periodicity. Dashed lines mark arrival times of major seismic phases (*Ps*, orange; *Pbs*, blue; *Pbp*, red). **b-c**, Same as **a** for stations **MA03** and **WAIS**, respectively.

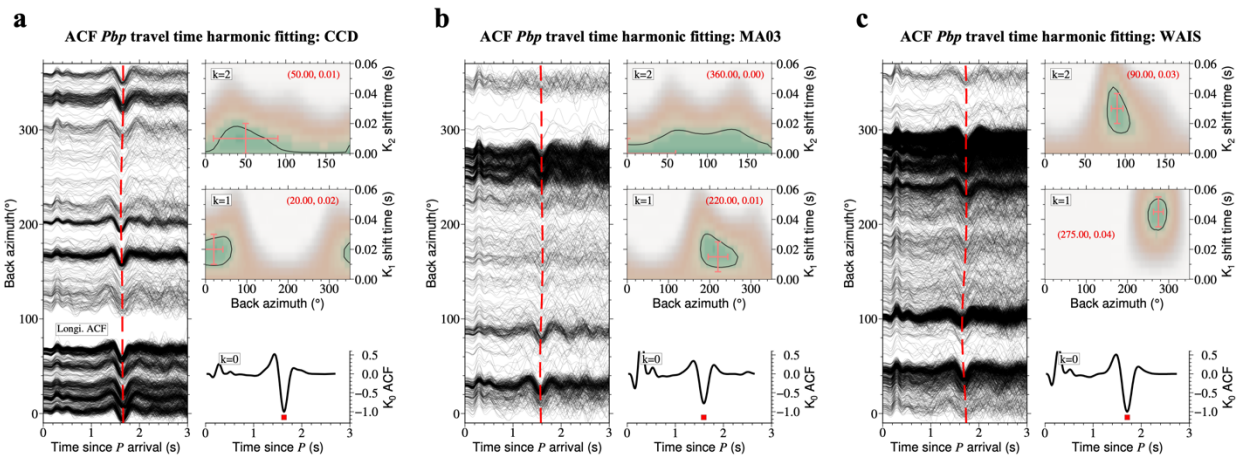

Supplementary Fig. 2 | Harmonic fitting for azimuth-dependent *Pbp* travel times from ACFs at representative Antarctic seismic stations. a, Station **CCD** (Dome C., East Antarctica). Left, individual longitudinal (longi.) ACFs (black lines) as a function of tele-seismic back-azimuth, along with the best-fitting azimuthally varying *Pbp* travel time (red line). Right, maximum ACF amplitude (colored background) as a function of back-azimuth and shift time: for K_2 (π back-azimuthal periodicity; top) and K_1 (2π periodicity; middle); and the stacked isotropic (K_0) ACF waveform (bottom). Red crosses denote optimal back-azimuths and shift times for each harmonic, with uncertainties shown by error bars. The red square marks the best-fitting isotropic *Pbp* travel time. **b-c**, Same as **a** for stations **MA03** and **WAIS** (West Antarctica), respectively.

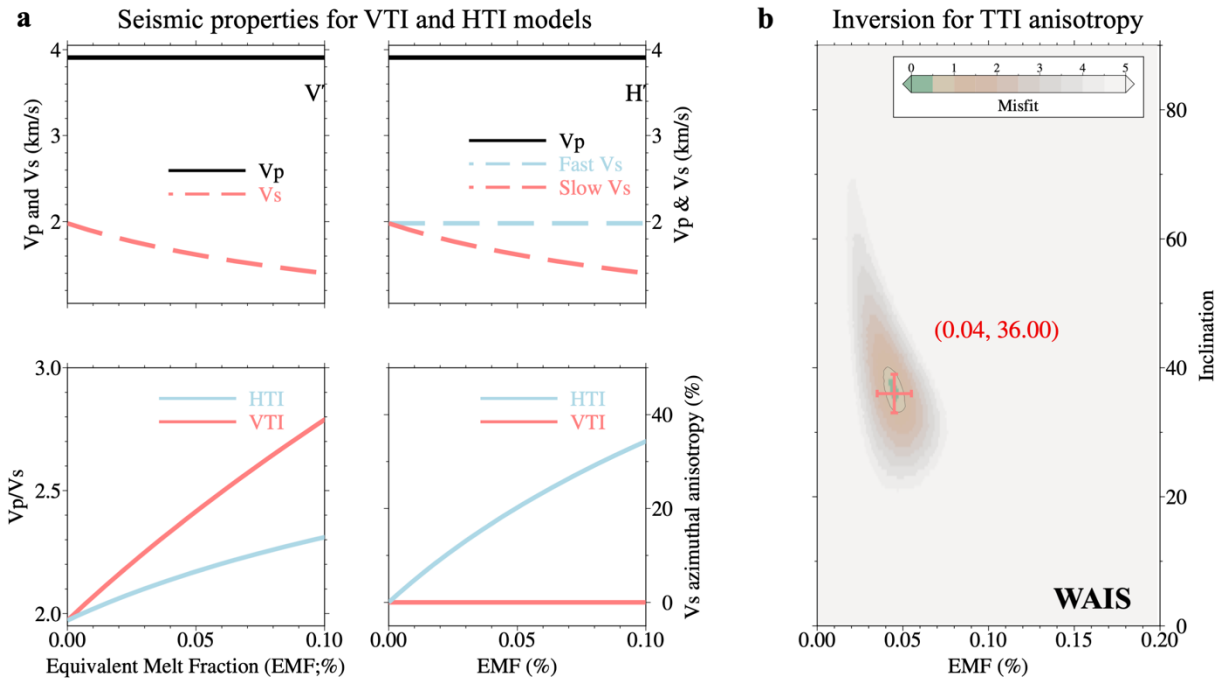

Supplementary Fig. 3 | Synthetic seismic properties of endmember models and inversion for lower-ice TTI anisotropy parameters. a, Synthetic *P*- and *S*-wave velocities for vertical transverse isotropy (VTI; top left) and horizontal transverse isotropy (HTI; top right) models as functions of equivalent melt fraction (EMF), together with corresponding *Vp/Vs* ratios (bottom left) and *Vs* azimuthal anisotropy (bottom right). **b,** Misfit (colored background) as a function of EMF and grain c-axes inclination from a grid search, with the best-fitting solution indicated by the red cross. Results are shown for station **WAIS**.

Supplementary Table 1: Detailed information for 181 seismic stations in study region

Network	Station	Longitude (deg.)	Latitude (deg.)	Start time	End time
IU	CASY	110.53540	-66.27920	1996-02-19T	2599-12-31T
IU	QSPA	145.00000	-89.92700	2003-01-01T	2599-12-31T
IU	PMSA	-64.04890	-64.77440	1993-03-03T	2599-12-31T
IU	SBA	166.75720	-77.84920	1998-10-28T	2599-12-31T
ZJ	APRL	158.70343	-73.19486	2012-11-20T	2015-11-18T
ZJ	BEBP	156.86902	-73.03255	2012-12-03T	2015-11-17T
ZJ	CASY	159.63188	-73.29592	2012-11-19T	2015-11-19T
ZJ	DONT	165.12001	-73.87685	2012-11-28T	2015-11-22T
ZJ	DUBY	158.07732	-74.98532	2012-11-25T	2015-11-14T
ZJ	FOOT	157.85344	-73.09341	2012-01-01T	2016-01-01T
ZJ	GRAW	154.98865	-74.00416	2012-11-18T	2015-11-14T
ZJ	KNYN	153.32700	-76.23735	2012-11-18T	2015-11-15T
ZJ	LEON	163.32777	-73.71343	2012-12-03T	2015-11-22T
ZJ	MICH	164.09976	-73.81710	2012-12-02T	2015-11-22T
ZJ	RAPH	162.28847	-73.59729	2012-11-30T	2015-11-21T
ZJ	RKST	159.00176	-74.20106	2012-11-22T	2015-11-13T
ZJ	SAMH	153.99675	-75.20303	2012-11-16T	2015-11-21T
ZJ	SHRD	160.49884	-73.39894	2012-12-05T	2015-11-25T
ZJ	SPLN	161.47122	-73.46622	2012-12-05T	2015-11-25T
XP	ARHT	166.66084	-77.83728	2000-12-16T	2003-12-31T
XP	CASE	160.10330	-80.44050	2001-12-06T	2003-12-31T
XP	CBOB	163.17119	-77.03478	2000-12-08T	2003-12-31T
XP	CBRI	166.42660	-77.25160	2002-01-30T	2003-12-31T
XP	CCRZ	169.09447	-77.51666	2001-11-20T	2003-12-31T
XP	CPHI	162.64877	-75.07452	2001-11-29T	2003-12-31T
XP	CTEA	160.76410	-78.94395	2001-11-22T	2003-12-31T
XP	DIHI	159.48004	-79.84902	2000-12-13T	2003-12-31T
XP	E000	163.61765	-77.62629	2001-11-20T	2003-12-31T
XP	E002	163.00893	-77.57506	2001-11-25T	2003-12-31T
XP	E004	162.06613	-77.41325	2000-12-14T	2003-12-31T
XP	E006	161.62570	-77.37020	2002-01-23T	2003-12-31T
XP	E008	160.56148	-77.28017	2000-12-18T	2003-12-31T
XP	E010	160.08644	-77.18473	2001-11-28T	2003-12-31T
XP	E012	159.32597	-77.04611	2001-11-20T	2003-12-31T
XP	E014	158.62321	-76.98998	2001-11-16T	2003-12-31T

Network	Station	Longitude (deg.)	Latitude (deg.)	Start time	End time
XP	E018	157.22368	-76.82340	2001-11-16T	2003-12-31T
XP	E020	156.54721	-76.72949	2001-11-26T	2003-12-31T
XP	E022	155.90346	-76.62801	2001-11-26T	2003-12-31T
XP	E024	155.23779	-76.53936	2001-11-26T	2003-12-31T
XP	E026	154.75906	-76.42470	2001-11-28T	2003-12-31T
XP	E028	154.03935	-76.30746	2001-11-27T	2003-12-31T
XP	E030	153.37918	-76.25106	2000-12-11T	2003-12-31T
XP	JNCT	157.90083	-76.93131	2000-12-11T	2003-12-31T
XP	MAGL	162.40834	-76.13807	2001-11-21T	2003-12-31T
XP	MCMD	166.67444	-77.84768	2002-02-06T	2003-12-31T
XP	MINN	166.88007	-78.55045	2001-12-03T	2003-12-31T
XP	N000	160.37845	-76.00875	2001-12-04T	2003-12-31T
XP	N020	155.81798	-77.46777	2001-11-15T	2003-12-31T
XP	N028	153.65086	-78.02958	2001-11-18T	2003-12-31T
XP	N036	151.27841	-78.55080	2000-12-12T	2003-12-31T
XP	N044	148.61592	-79.06919	2001-11-21T	2003-12-31T
XP	N052	145.74890	-79.54412	2001-11-21T	2003-12-31T
XP	N060	142.59500	-80.00010	2001-12-07T	2003-12-31T
XP	N068	138.91589	-80.39280	2002-12-09T	2003-12-31T
XP	N076	135.43401	-80.80620	2001-12-08T	2003-12-31T
XP	N084	131.46899	-81.16020	2001-12-07T	2003-12-31T
XP	N092	126.97970	-81.45930	2001-12-04T	2003-12-31T
XP	N100	122.61000	-81.65250	2001-12-02T	2003-12-31T
XP	N108	117.60520	-81.87950	2001-12-03T	2003-12-31T
XP	N116	112.57120	-82.00980	2001-12-05T	2003-12-31T
XP	N124	107.64250	-82.07420	2001-12-08T	2003-12-31T
XP	N132	101.95570	-82.07520	2001-12-05T	2003-12-31T
XP	RIS0	172.49883	-78.08321	2000-12-07T	2003-12-31T
XP	TIMW	135.26950	-80.39120	2001-12-08T	2003-12-31T
1D	ATOL	-68.87012	-71.38967	2017-01-10T	2018-01-29T
1D	BREN	-63.02094	-72.67498	2017-01-19T	2018-01-17T
1D	ELSW	-85.70758	-75.51937	2017-01-06T	2018-01-21T
1D	FOSS	-68.30544	-71.31456	2016-01-13T	2017-01-10T
1D	FOWL	-79.30112	-76.89284	2016-02-13T	2018-01-14T
1D	KEAL	-85.69965	-76.52038	2016-02-07T	2017-01-06T
1D	KIBB	-65.60490	-75.27611	2016-01-16T	2018-02-08T
1D	PIG1	-97.57499	-73.97827	2016-01-28T	2018-01-23T
1D	PIG2	-97.68297	-74.45573	2016-01-29T	2016-12-25T

Network	Station	Longitude (deg.)	Latitude (deg.)	Start time	End time
1D	PIG3	-97.47445	-75.08406	2016-01-30T	2018-01-23T
1D	PIG4	-97.58304	-75.75994	2016-01-30T	2016-12-21T
1D	PIGD	-100.27585	-75.80261	2016-01-31T	2018-01-25T
1D	ROTH	-68.14885	-67.52001	2016-01-12T	2017-01-14T
1D	S001	-154.10001	-84.50000	2010-11-25T	2010-12-31T
1D	S003	-157.50000	-84.60000	2010-11-25T	2010-12-31T
1D	S008	-157.70000	-84.48000	2010-11-25T	2010-12-31T
1D	S009	-156.10001	-84.51000	2010-11-25T	2010-12-31T
1D	S010	-158.12500	-84.33000	2010-11-25T	2010-12-31T
1D	S011	-155.50000	-84.30000	2010-11-25T	2010-12-31T
1D	WELC	-63.82737	-70.73181	2017-01-18T	2018-01-06T
ZM	AGO1	129.61211	-83.85960	2007-12-01T	2012-12-15T
ZM	AGO3	28.58340	-82.75400	2009-12-31T	2012-12-02T
ZM	ALYS	-23.73420	-84.35490	2012-01-16T	2012-10-17T
ZM	GM01	104.72910	-83.98580	2007-12-14T	2009-12-31T
ZM	GM02	97.58150	-79.42510	2008-12-23T	2011-12-31T
ZM	GM03	85.94390	-80.21690	2009-01-04T	2009-12-23T
ZM	GM04	61.11240	-82.99970	2007-12-26T	2009-12-19T
ZM	GM05	51.15880	-81.18410	2008-12-29T	2012-12-31T
ZM	GM06	44.31480	-79.33280	2009-01-04T	2009-12-29T
ZM	GM07	39.61320	-77.31360	2009-01-05T	2013-01-01T
ZM	N100	122.59010	-81.65170	2010-01-01T	2012-12-31T
ZM	N124	107.64060	-82.07450	2007-12-16T	2009-12-21T
ZM	N132	101.95340	-82.07510	2008-12-22T	2009-12-21T
ZM	N140	96.76920	-82.00860	2007-12-27T	2012-12-27T
ZM	N148	91.50760	-81.86250	2008-12-24T	2009-12-24T
ZM	N156	86.50450	-81.67260	2007-12-28T	2009-12-23T
ZM	N165	81.76040	-81.40840	2008-12-26T	2009-12-24T
ZM	N173	77.47360	-81.11220	2007-12-17T	2009-12-20T
ZM	N182	73.18980	-80.73630	2008-12-27T	2009-12-20T
ZM	N190	69.43100	-80.32750	2008-12-24T	2009-12-24T
ZM	N198	65.96070	-79.85970	2007-12-14T	2009-12-28T
ZM	N206	62.85560	-79.39470	2009-01-01T	2009-12-21T
ZM	N215	59.99430	-78.90450	2009-01-01T	2011-09-17T
ZM	P061	77.22380	-84.49960	2007-12-26T	2012-12-15T
ZM	P071	77.33470	-83.64650	2008-12-26T	2009-12-24T
ZM	P080	77.36400	-82.80540	2007-12-17T	2009-12-22T
ZM	P090	77.31420	-81.93610	2009-01-04T	2009-12-24T

Network	Station	Longitude (deg.)	Latitude (deg.)	Start time	End time
ZM	P116	77.04510	-79.56690	2008-12-26T	2009-12-24T
ZM	P124	77.65700	-78.87180	2008-12-27T	2010-01-08T
G	CCD	123.30500	-75.10650	2010-01-01T	2015-01-01T
YT	BYRD	-119.47380	-80.01700	2010-01-13T	2023-08-17T
YT	AGO1	129.61520	-83.86150	2012-12-15T	2017-12-31T
YT	AGO3	28.58100	-82.75410	2012-12-02T	2017-12-31T
YT	ALYS	-23.73470	-84.35480	2012-12-28T	2017-12-31T
YT	BEAR	-111.85110	-74.54760	2011-01-14T	2023-12-01T
YT	BENN	-117.39230	-84.57310	2010-12-17T	2022-08-23T
YT	CLRK	-141.84850	-77.32310	2010-01-05T	2017-12-31T
YT	DEVL	161.97300	-81.47550	2008-12-15T	2018-12-31T
YT	DNTW	-107.77690	-76.45120	2010-01-02T	2023-12-25T
YT	DUFK	-53.20060	-82.86190	2007-01-15T	2020-12-31T
YT	EAGL	-22.30980	-80.89440	2016-01-22T	2018-01-18T
YT	FALL	-143.62840	-85.30660	2009-12-29T	2019-12-31T
YT	FISH	162.56520	-78.92760	2009-01-20T	2017-12-31T
YT	GM05	51.15870	-81.18410	2010-10-12T	2013-12-31T
YT	HOWD	-86.76940	-77.52860	2008-01-09T	2023-11-24T
YT	KOLR	-120.72700	-76.15440	2010-01-18T	2018-12-31T
YT	LONW	152.73500	-81.34660	2008-01-29T	2018-12-31T
YT	LPLY	-90.28340	-73.11420	2018-12-22T	2023-12-15T
YT	MA01	-97.55960	-76.93970	2015-01-07T	2018-01-31T
YT	MA02	-97.55950	-77.43940	2015-01-08T	2016-12-31T
YT	MA03	-97.55850	-77.94010	2015-01-08T	2016-12-31T
YT	MA04	-97.58790	-78.42210	2015-01-10T	2016-12-31T
YT	MA05	-97.55730	-78.93950	2015-01-11T	2016-12-31T
YT	MA06	-97.55870	-79.43970	2015-01-12T	2016-12-31T
YT	MA07	-93.49910	-78.24960	2015-01-10T	2016-12-31T
YT	MA08	-103.00220	-77.40140	2015-01-06T	2016-12-31T
YT	MA09	-104.99770	-79.89930	2015-01-13T	2016-12-31T
YT	MA10	-109.00030	-78.59990	2014-12-22T	2016-12-31T
YT	MCRG	-94.64930	-73.66810	2019-01-01T	2023-12-23T
YT	MECK	-72.18500	-75.28080	2008-01-08T	2019-01-31T
YT	MILR	156.25170	-83.30630	2008-02-10T	2017-12-31T
YT	MPAT	-155.02210	-78.02970	2007-12-18T	2017-12-31T
YT	MTAK	-112.79860	-76.31570	2019-01-07T	2023-11-30T
YT	N140	96.75580	-82.01040	2012-12-27T	2017-12-31T
YT	P061	77.22430	-84.49970	2012-12-18T	2017-12-31T

Network	Station	Longitude (deg.)	Latitude (deg.)	Start time	End time
YT	PECA	-68.55250	-85.61240	2008-01-15T	2020-12-31T
YT	RMBO	-66.39590	-83.87140	2014-01-06T	2020-12-31T
YT	SILY	-125.96600	-77.13320	2010-01-06T	2018-12-31T
YT	SIPL	-148.95530	-81.64050	2007-12-17T	2017-12-31T
YT	ST01	-98.74180	-83.22800	2010-01-27T	2012-12-31T
YT	ST02	-109.12470	-82.06900	2010-01-20T	2012-12-31T
YT	ST03	-113.15080	-81.40650	2010-01-20T	2012-12-31T
YT	ST04	-116.57920	-80.71520	2010-01-17T	2012-12-31T
YT	ST06	-121.82010	-79.33170	2010-01-17T	2012-12-31T
YT	ST07	-123.79530	-78.63880	2010-01-16T	2012-12-31T
YT	ST08	-125.53130	-77.94760	2010-01-17T	2012-12-31T
YT	ST09	-128.47340	-76.53090	2010-01-17T	2012-12-31T
YT	ST10	-129.74890	-75.81430	2010-01-21T	2012-12-31T
YT	ST12	-123.81600	-76.89700	2010-01-17T	2012-12-31T
YT	ST13	-130.51390	-77.56090	2010-01-18T	2012-12-31T
YT	ST14	-134.08020	-77.83780	2010-01-18T	2012-12-31T
YT	STEW	-86.23490	-84.18630	2014-01-08T	2020-12-31T
YT	SURP	-171.20170	-84.71990	2008-02-09T	2018-12-31T
YT	THRO	-28.31750	-79.12730	2016-02-06T	2017-03-29T
YT	THUR	-97.56060	-72.53010	2011-01-19T	2023-12-14T
YT	UNGL	-82.52400	-79.77460	2010-12-28T	2023-12-05T
YT	UPTW	-109.03740	-77.57810	2011-01-26T	2020-12-31T
YT	WAIS	-111.77790	-79.41810	2009-02-05T	2024-01-20T
YT	WAWA	-28.42070	-81.57840	2014-01-16T	2018-12-31T
YT	WHIT	-104.38670	-82.68230	2010-01-19T	2023-11-26T
YT	WILS	-80.55870	-80.03960	2008-01-08T	2010-12-31T
YT	WNDY	-119.41350	-82.36950	2010-01-27T	2010-12-31T
5F	CAS04	120.22574	-75.71610	2010-01-15T	2011-12-24T
5F	CAS05	116.96767	-76.34698	2011-01-15T	2011-12-28T
5F	CAS06	112.98671	-76.84097	2010-01-25T	2011-12-31T
5F	CAS07	110.54959	-77.67788	2010-01-27T	2011-12-31T
5F	CAS08	107.11978	-78.40895	2010-01-16T	2011-12-31T

Supplementary Table 2: Observed *PbP* arrival times from ACF

Station ID	Zero-order component (K_0, s)	First-order component (K_1, s)	First-order component back-azimuth (θ_1, deg.)	Second-order component (K_2, s)	Second-order component back-azimuth (θ_2, deg.)
1D.ELSW	1.03	0.04	320	0.01	10
1D.KEAL	1.18	0.02	120	0.01	120
1D.PIG4	0.90	0.01	50	0.01	170
5F.CAS04	1.77	0.01	340	0.00	120
5F.CAS05	1.82	0.03	90	0.01	150
5F.CAS06	1.70	0.02	310	0.01	30
5F.CAS07	1.63	0.01	140	0.01	160
5F.CAS08	1.87	0.03	280	0.01	150
G.CCD	1.63	0.02	20	0.01	50
IU.QSPA	1.70	0.11	100	0.02	120
XP.E012	0.99	0.18	310	0.07	140
XP.E018	0.94	0.01	100	0.03	60
XP.E020	1.01	0.01	260	0.02	80
XP.E024	0.92	0.02	190	0.01	30
XP.E026	1.00	0.01	120	0.01	40
XP.E028	0.73	0.02	220	0.02	80
XP.E030	1.51	0.17	160	0.07	60
XP.N020	0.94	0.03	140	0.01	130
XP.N028	1.40	0.01	30	0.09	90
XP.N036	1.65	0.17	40	0.05	90
XP.N044	1.11	0.03	320	0.01	170
XP.N052	1.32	0.07	150	0.10	100
XP.N060	1.59	0.01	50	0.01	40
XP.N068	1.60	0.08	60	0.06	20
XP.N076	1.30	0.00	300	0.02	10
XP.N084	1.27	0.02	90	0.02	30
XP.N092	1.36	0.01	170	0.01	10
XP.N100	1.31	0.02	240	0.00	120
XP.N108	1.31	0.01	10	0.00	120
XP.N116	1.11	0.02	270	0.02	40
XP.N124	1.27	0.02	260	0.01	130
XP.N132	1.71	0.02	100	0.00	120
XP.TIMW	1.35	0.00	300	0.01	20
YT.AGO1	1.62	0.00	300	0.00	120

Station ID	Zero-order component (K_0, s)	First-order component (K_1, s)	First-order component back-azimuth (θ_1, deg.)	Second-order component (K_2, s)	Second-order component back-azimuth (θ_2, deg.)
YT.AGO3	1.01	0.00	300	0.00	120
YT.BENN	0.84	0.02	30	0.00	120
YT.BYRD	1.13	0.01	30	0.00	120
YT.GM05	1.48	0.04	300	0.02	0
YT.KOLR	1.28	0.08	120	0.03	20
YT.MA01	1.04	0.01	300	0.02	70
YT.MA02	1.66	0.01	200	0.02	90
YT.MA03	1.59	0.02	200	0.01	60
YT.MA04	1.68	0.03	60	0.01	90
YT.MA05	1.65	0.02	80	0.00	120
YT.MA06	2.33	0.06	230	0.01	130
YT.MA07	1.83	0.10	270	0.02	90
YT.MA08	1.64	0.00	300	0.01	70
YT.MA09	1.49	0.01	310	0.01	90
YT.MA10	0.96	0.02	350	0.00	120
YT.N140	1.24	0.07	220	0.02	130
YT.P061	1.53	0.03	20	0.03	70
YT.ST01	1.53	0.00	300	0.02	60
YT.ST03	1.01	0.02	330	0.02	80
YT.ST04	1.79	0.02	160	0.03	90
YT.ST06	1.49	0.01	330	0.01	110
YT.ST07	1.30	0.02	20	0.02	100
YT.ST08	1.28	0.03	350	0.01	120
YT.ST09	1.62	0.04	130	0.04	60
YT.ST10	0.95	0.03	130	0.02	170
YT.ST13	1.27	0.03	50	0.01	80
YT.ST14	0.83	0.00	300	0.03	110
YT.UPTW	1.50	0.04	190	0.03	70
YT.WAIS	1.71	0.04	270	0.02	90
YT.WNDY	0.93	0.03	150	0.00	120
ZJ.APRL	1.47	0.01	220	0.01	0
ZJ.BEBP	1.49	0.00	300	0.00	120
ZJ.CASY	0.93	0.03	160	0.07	140
ZJ.FOOT	1.19	0.00	300	0.02	150
ZJ.GRAW	1.25	0.03	340	0.03	0
ZJ.KNYN	1.09	0.02	240	0.02	140

Station ID	Zero-order component (K_0, s)	First-order component (K_1, s)	First-order component back-azimuth (θ_1, deg.)	Second-order component (K_2, s)	Second-order component back-azimuth (θ_2, deg.)
ZJ.SAMH	1.47	0.06	40	0.04	170
ZM.AGO1	1.62	0.01	110	0.01	50
ZM.AGO3	1.01	0.00	300	0.00	120
ZM.GM01	1.58	0.02	350	0.02	40
ZM.GM02	1.54	0.02	90	0.01	30
ZM.GM03	1.64	0.08	280	0.07	140
ZM.GM04	1.67	0.02	50	0.02	150
ZM.GM05	1.48	0.04	300	0.01	10
ZM.GM06	1.65	0.01	230	0.01	120
ZM.GM07	1.55	0.02	250	0.01	130
ZM.N100	1.31	0.02	260	0.00	120
ZM.N124	1.28	0.02	250	0.00	120
ZM.N132	1.72	0.02	90	0.00	120
ZM.N140	1.23	0.06	210	0.02	110
ZM.N148	1.63	0.05	290	0.00	120
ZM.N156	1.23	0.04	270	0.03	50
ZM.N165	1.40	0.07	310	0.04	50
ZM.N173	1.30	0.03	130	0.04	70
ZM.N182	1.41	0.01	220	0.00	120
ZM.N190	1.62	0.06	160	0.02	100
ZM.N198	1.35	0.04	130	0.02	0
ZM.N206	1.21	0.05	230	0.01	150
ZM.N215	1.50	0.02	160	0.01	120
ZM.P061	1.52	0.01	40	0.01	50
ZM.P071	1.08	0.01	0	0.00	120
ZM.P080	1.33	0.01	230	0.01	170
ZM.P116	0.97	0.04	310	0.02	50
ZM.P124	0.83	0.04	100	0.01	100

106 **Supplementary Table 3: MCMC parameters in inversion for 2D seismic structure**

Parameters	Bound	Max. jump	Step	Initial models
Ice thickness (km)	$0.5h$ – $1.5h$	0.5	0.05	h
Ice *Vs* (km/s)	1.0 – 2.2	0.1	0.02	2.0
Ice anisotropy strength (%)	0.0 – 30.0	5.0	0.1	0.0
Ice fast velocity direction (°)	0.0 – 180.0	30.0	1.0	90.0
Interface dip angle (°)	0.0 – 30.0	5.0	0.5	0.0
Interface dip azimuth (°)	0.0 – 360.0	30.0	1.0	180.0
Crust *Vs* (km/s)	$0.1m$ – $1.5m$	0.2	0.02	m

h denotes ice thickness estimated from *Pbp* travel time
m represents the average *Vs* within the topmost 6 km of the upper crust, as derived from the Shen18 model[2] or a default value of 3.2 km/s for seismic stations not covered by the Shen18 model

107

Supplementary Table 4: Bulk-ice seismic structures across stations

Station ID	Ice thickness (km)	Thickness uncertainty (km)	*Vp*/*Vs*	*Vp*/*Vs* uncertainty	Dip (°)	Dip uncertainty (°)	Dip baz. (°)	Dip baz. uncertainty (°)	Anisotropy strength (%)	Anisotropy strength uncertainty (%)	Anisotropy baz. (°)	Anisotropy baz. uncertainty (°)
1D.ATOL	0.86	0.08	2.18	0.17	1.24	0.74	136	66	NaN	NaN	NaN	NaN
1D.ELSW	1.91	0.02	2.25	0.05	2.18	0.45	326	12	3.4	1.3	20	11
1D.FOWL	0.77	0.03	2.13	0.09	5.34	0.86	99	6	8.2	3.0	124	11
1D.KEAL	2.18	0.03	2.29	0.08	2.68	0.54	65	9	3.7	1.8	82	20
1D.PIG1	0.49	0.06	3.02	0.33	3.10	0.79	196	16	5.8	2.6	70	17
1D.PIG3	0.68	0.08	3.04	0.29	0.98	0.57	15	55	3.4	1.5	74	24
1D.PIG4	1.65	0.02	2.26	0.05	3.35	0.44	75	5	2.1	0.9	63	27
1D.PIGD	0.87	0.05	3.33	0.20	1.05	0.42	175	26	3.2	1.4	90	23
5F.CAS04	3.26	0.04	2.35	0.06	0.99	0.65	251	94	6.0	2.2	52	12
5F.CAS05	3.34	0.04	2.26	0.05	1.87	0.81	76	31	NaN	NaN	NaN	NaN
5F.CAS06	3.17	0.03	2.19	0.05	2.86	0.71	208	15	NaN	NaN	NaN	NaN
5F.CAS07	3.05	0.03	2.20	0.04	1.71	0.64	173	28	NaN	NaN	NaN	NaN
5F.CAS08	3.49	0.04	2.20	0.05	3.36	0.78	255	14	NaN	NaN	NaN	NaN
G.CCD	3.05	0.02	2.20	0.04	1.08	0.58	233	40	2.5	1.1	142	26
IU.QSPA	3.15	0.09	2.01	0.07	0.79	0.54	82	65	3.3	1.1	66	11
XP.E018	1.77	0.02	2.18	0.05	0.92	0.62	47	43	2.4	1.1	112	29
XP.E030	2.33	0.05	2.02	0.06	3.41	0.61	87	3	NaN	NaN	NaN	NaN
XP.N036	2.70	0.13	2.25	0.12	1.49	0.61	16	32	2.9	1.1	153	14
XP.N060	2.94	0.04	2.68	0.08	1.24	0.75	175	91	5.0	2.1	29	15
XP.N068	2.97	0.03	2.12	0.04	0.62	0.46	80	81	NaN	NaN	NaN	NaN
XP.N076	2.39	0.03	2.22	0.04	0.80	0.49	141	46	5.9	1.5	157	6
XP.N084	2.38	0.03	2.19	0.05	2.00	0.64	78	16	2.5	1.2	18	36

Station ID	Ice thickness (km)	Thickness uncertainty (km)	*Vp*/*Vs*	*Vp*/*Vs* uncertainty	Dip (°)	Dip uncertainty (°)	Dip baz. (°)	Dip baz. uncertainty (°)	Anisotropy strength (%)	Anisotropy strength uncertainty (%)	Anisotropy baz. (°)	Anisotropy baz. uncertainty (°)
XP.N092	2.55	0.02	2.19	0.04	1.36	0.45	182	20	2.0	1.0	47	36
XP.N100	2.45	0.02	2.23	0.04	0.90	0.37	216	28	2.0	0.9	142	27
XP.N108	2.45	0.03	2.21	0.05	1.10	0.52	319	39	3.0	1.4	10	25
XP.N116	2.11	0.02	2.09	0.03	0.96	0.48	238	42	NaN	NaN	NaN	NaN
XP.N124	2.33	0.03	2.23	0.05	3.31	0.45	276	7	5.1	1.4	57	8
XP.N132	3.22	0.03	2.20	0.03	2.11	0.47	133	12	1.8	0.9	78	37
XP.TIMW	2.48	0.03	2.19	0.05	1.76	0.59	147	23	6.3	1.8	158	8
YT.AGO1	3.01	0.03	2.24	0.03	0.81	0.45	278	54	3.9	1.3	169	7
YT.AGO3	1.90	0.02	2.10	0.04	1.07	0.46	123	33	2.5	1.1	2	19
YT.BYRD	2.13	0.02	2.14	0.04	2.12	0.44	11	12	3.5	1.4	164	19
YT.GM05	2.74	0.03	2.07	0.03	2.31	0.54	272	14	NaN	NaN	NaN	NaN
YT.MA01	1.95	0.02	2.10	0.03	1.86	0.47	307	16	2.4	1.0	21	13
YT.MA02	3.11	0.03	2.38	0.07	1.02	0.63	355	67	2.7	1.3	94	37
YT.MA03	2.96	0.03	2.13	0.04	3.58	0.58	231	9	4.4	1.4	139	10
YT.MA04	3.14	0.02	2.15	0.03	3.78	0.54	33	8	2.8	1.1	137	17
YT.MA06	4.37	0.03	2.37	0.04	0.94	0.52	228	47	2.6	0.9	95	14
YT.MA07	3.44	0.11	2.24	0.09	3.19	0.61	279	11	5.7	1.6	90	8
YT.MA09	2.80	0.03	2.23	0.04	0.40	0.40	339	90	1.7	1.0	91	49
YT.MA10	1.76	0.02	2.19	0.04	3.16	0.50	24	8	3.7	1.1	109	11
YT.N140	2.32	0.02	2.22	0.05	4.22	0.52	236	6	2.2	1.1	96	23
YT.P061	2.87	0.02	2.15	0.04	0.86	0.49	35	46	2.1	1.0	89	32
YT.ST01	2.84	0.02	2.12	0.03	1.32	0.53	37	26	3.8	1.1	29	10
YT.ST02	2.49	0.08	2.25	0.10	2.97	0.57	194	11	7.4	1.8	151	6
YT.ST03	1.86	0.02	2.14	0.03	0.86	0.43	339	36	1.5	0.8	143	45
YT.ST04	3.32	0.03	2.60	0.05	1.22	0.72	155	50	3.9	1.4	131	13

Station ID	Ice thickness (km)	Thickness uncertainty (km)	*Vp*/*Vs*	*Vp*/*Vs* uncertainty	Dip (°)	Dip uncertainty (°)	Dip baz. (°)	Dip baz. uncertainty (°)	Anisotropy strength (%)	Anisotropy strength uncertainty (%)	Anisotropy baz. (°)	Anisotropy baz. uncertainty (°)
YT.ST06	2.78	0.03	2.71	0.06	0.93	0.58	249	78	2.8	1.2	125	25
YT.ST08	2.36	0.03	2.37	0.07	3.05	0.59	34	11	6.5	2.0	42	10
YT.ST10	1.72	0.03	2.12	0.04	2.26	0.62	135	15	7.4	1.8	7	5
YT.ST13	2.34	0.02	2.12	0.04	2.81	0.57	29	11	5.2	1.4	77	8
YT.ST14	1.49	0.02	2.21	0.04	1.61	0.51	73	15	3.5	1.1	99	9
YT.UPTW	2.81	0.03	2.54	0.06	3.19	0.70	177	13	2.8	1.3	104	27
YT.WAIS	3.17	0.03	2.18	0.03	2.08	0.52	253	14	4.8	1.3	99	8
YT.WNDY	1.72	0.02	2.20	0.04	3.19	0.44	122	7	2.3	1.0	37	22
ZJ.APRL	2.75	0.03	2.30	0.05	2.29	0.55	238	15	2.1	1.1	5	66
ZJ.BEBP	2.81	0.03	2.12	0.04	2.16	0.48	50	12	2.4	1.1	70	21
ZJ.KNYN	2.07	0.02	2.04	0.03	3.10	0.52	120	8	2.9	0.9	131	11
ZM.GM01	2.97	0.02	2.21	0.04	0.34	0.36	135	109	2.0	1.0	67	38
ZM.GM02	2.88	0.03	2.15	0.05	2.16	0.61	164	18	2.9	1.4	34	31
ZM.GM03	3.04	0.03	2.11	0.04	2.61	0.53	264	12	4.5	1.4	117	11
ZM.GM04	3.13	0.03	2.07	0.04	1.19	0.50	168	30	2.3	1.1	69	40
ZM.N148	3.05	0.03	2.35	0.08	2.07	0.59	322	15	3.2	1.6	65	30
ZM.N156	2.28	0.03	2.21	0.05	3.29	0.52	309	8	5.3	1.5	46	9
ZM.N165	2.63	0.03	2.25	0.08	2.71	0.54	313	12	3.0	1.5	78	26
ZM.N173	2.41	0.03	2.21	0.05	3.48	0.50	124	7	4.3	1.5	78	12
ZM.N182	2.63	0.02	2.04	0.03	2.38	0.52	184	13	2.4	1.1	123	42
ZM.N190	3.03	0.03	2.23	0.04	2.23	0.47	168	13	3.4	1.4	23	16
ZM.N198	2.53	0.03	2.27	0.07	1.20	0.53	340	36	4.1	1.5	40	13
ZM.N206	2.27	0.02	2.17	0.04	1.25	0.42	220	24	2.3	1.1	50	30
ZM.N215	2.80	0.03	2.16	0.04	1.92	0.51	181	16	2.7	1.2	112	27
ZM.P071	2.02	0.02	2.17	0.04	0.53	0.39	38	54	4.6	1.2	121	8

Station ID	Ice thickness (km)	Thickness uncertainty (km)	*Vp*/*Vs*	*Vp*/*Vs* uncertainty	Dip (°)	Dip uncertainty (°)	Dip baz. (°)	Dip baz. uncertainty (°)	Anisotropy strength (%)	Anisotropy strength uncertainty (%)	Anisotropy baz. (°)	Anisotropy baz. uncertainty (°)
ZM.P080	2.49	0.03	2.04	0.05	2.33	0.62	210	18	2.6	1.3	52	34
ZM.P090	2.42	0.07	2.08	0.07	2.52	0.55	69	9	6.1	1.8	129	9
ZM.P124	1.41	0.02	2.20	0.04	5.22	0.63	62	5	16.7	2.1	122	3

Backazimuth is defined as the clockwise angle from geodetic north.
NaN indicates that no reliable estimate could be obtained.

110
111

Supplementary Table 5: Lower-ice seismic anisotropic structures across stations

Station ID	*Vp/Vs*	Anisotropy strength	Equivalent Melt Fraction (%)	Inclination (°)
XP.N076	2.34	0.083	0.054	37
ZJ.APRL	2.45	0.030	0.060	20
YT.ST06	3.06	0.037	0.151	15
XP.N124	2.35	0.072	0.054	34
5F.CAS05	2.40	NaN	0.048	NaN
YT.MA04	2.24	0.040	0.035	30
1D.FOWL	2.21	0.117	0.043	53
YT.ST01	2.20	0.054	0.032	38
XP.N132	2.31	0.026	0.041	22
1D.ATOL	2.28	NaN	0.033	NaN
XP.N108	2.32	0.043	0.045	28
5F.CAS07	2.32	NaN	0.038	NaN
ZM.N148	2.54	0.044	0.074	22
ZJ.BEBP	2.19	0.034	0.029	31
ZM.P124	2.32	0.235	0.077	64
YT.P061	2.24	0.030	0.033	27
YT.BYRD	2.22	0.051	0.034	35
ZM.N190	2.36	0.048	0.051	28
ZM.P090	2.13	0.088	0.029	56
1D.PIG4	2.40	0.030	0.054	21
5F.CAS08	2.31	NaN	0.037	NaN
ZM.N215	2.25	0.039	0.036	29
XP.N092	2.30	0.029	0.040	24
ZJ.KNYN	2.07	0.043	0.016	49
YT.MA06	2.57	0.036	0.077	20
IU.QSPA	2.04	0.049	0.012	68
YT.ST02	2.39	0.103	0.064	39

Station ID	*Vp/Vs*	Anisotropy strength	Equivalent Melt Fraction (%)	Inclination (°)
YT.UPTW	2.82	0.038	0.113	17
YT.MA02	2.58	0.036	0.079	20
ZM.GM03	2.18	0.065	0.031	43
XP.N036	2.39	0.040	0.053	25
XP.N060	3.02	0.066	0.151	20
XP.N068	2.19	NaN	0.023	NaN
XP.TIMW	2.30	0.089	0.049	41
G.CCD	2.31	0.035	0.043	26
YT.ST14	2.33	0.050	0.048	29
ZM.P080	2.08	0.039	0.016	46
ZM.GM02	2.24	0.041	0.035	31
YT.N140	2.34	0.032	0.046	23
XP.E030	2.05	NaN	0.008	NaN
YT.MA07	2.38	0.080	0.058	35
ZM.N156	2.32	0.075	0.050	36
1D.PIG3	3.56	0.043	0.199	12
1D.KEAL	2.45	0.051	0.063	26
YT.WAIS	2.29	0.069	0.045	36
YT.GM05	2.12	NaN	0.016	NaN
5F.CAS04	2.53	0.082	0.080	30
ZM.N198	2.41	0.057	0.059	29
ZM.N173	2.32	0.061	0.048	33
1D.PIGD	3.98	0.039	0.199	2
XP.N116	2.15	NaN	0.019	NaN
YT.ST10	2.20	0.106	0.039	53
XP.N100	2.36	0.028	0.047	22
YT.AGO3	2.17	0.036	0.026	33
YT.ST04	2.91	0.052	0.129	19

Station ID	*Vp/Vs*	Anisotropy strength	Equivalent Melt Fraction (%)	Inclination (°)
XP.E018	2.29	0.033	0.040	26
YT.MA01	2.17	0.035	0.026	33
YT.MA10	2.29	0.052	0.043	32
YT.MA03	2.22	0.063	0.035	39
YT.ST03	2.22	0.022	0.030	24
ZM.GM01	2.32	0.028	0.043	22
YT.ST13	2.19	0.074	0.033	45
YT.WNDY	2.32	0.032	0.043	24
XP.N084	2.30	0.035	0.041	26
YT.MA09	2.36	0.024	0.046	20
ZM.N165	2.38	0.042	0.053	25
YT.AGO1	2.38	0.055	0.054	29
1D.PIG1	3.53	0.073	0.199	17
YT.ST08	2.56	0.089	0.085	31
ZM.N206	2.28	0.032	0.038	26
ZM.GM04	2.13	0.033	0.021	36
ZM.N182	2.08	0.035	0.016	44
5F.CAS06	2.30	NaN	0.035	NaN
1D.ELSW	2.39	0.048	0.054	27
ZM.P071	2.26	0.065	0.041	37

NaN indicates that no reliable estimate could be obtained.

113

114
115

References in Supplementary Information

1 Mouginot, J., Rignot, E. & Scheuchl, B. Continent - wide, interferometric SAR phase, mapping of Antarctic ice velocity. *Geophysical Research Letters* 46, 9710-9718 (2019).

2 Shen, W. *et al.* The crust and upper mantle structure of central and West Antarctica from Bayesian inversion of Rayleigh wave and receiver functions. *Journal of Geophysical Research: Solid Earth* 123, 7824-7849 (2018).